Appl Microbiol Biotechnol
DOI 10.1007/s00253-014-5770-z

Cloning, expression, and directed evolution of carbonyl reductase from *Leifsonia xyli* HS0904 with enhanced catalytic efficiency

Neng-Qiang Wang · Jing Sun · Jin Huang · Pu Wang

Received: 27 January 2014 / Revised: 9 April 2014 / Accepted: 10 April 2014
© Springer-Verlag Berlin Heidelberg 2014

Abstract (*R*)-[3,5-bis(trifluoromethyl)phenyl] ethanol ((*R*)-BTPE) is a valuable chiral intermediate for the synthesis of antiemetic drug Aprepitant and Fosaprepitant. A *Leifsonia xyli* HS0904-derived carbonyl reductase (LXCAR), an effective biocatalyst for the asymmetric reduction of 3,5-bis(trifluoromethyl) acetophenone (BTAP) to (*R*)-BTPE, was overexpressed in *Escherichia coli* BL21 (DE3). Bioinformatics analysis indicated that the amino acid sequence of recombinant LXCAR showed 89 % similarity to short-chain dehydrogenase/reductase. *E. coli* recombinant carbonyl reductase crude extract showed a specific activity of 1.54 U/mg, which was 62 times higher than that of *L. xyli* HS0904 crude extract. By using error-prone polymerase chain reaction and site-directed mutagenesis, the engineered LXCAR demonstrated superior catalytic activity toward BTAP, and the obtained mutant LXCAR-S154Y exhibited nearly 13-fold, 5.4-fold, and 2.3-fold increase in k_{cat}/K_m value, k_{cat} value, and specific activity toward BTAP, respectively, compared to the recombinant LXCAR. Additionally, the reduction of BTAP by whole cells of mutant LXCAR-S154Y afforded a best yield of 99.6 % for (*R*)-BTPE within 2 h at 200 mM BTAP, which was shortened by 28 and 2 h compared to those catalyzed by *L. xyli* HS0904 cells and recombinant *E. coli* cells expressing LXCAR, respectively. Moreover, a yield of 82.5 % for (*R*)-BTPE was achieved within 12 h at an increased BTAP concentration of up to 1,000 mM (256 g/l), representing a 1.9-fold increase over the recombinant LXCAR. Homology modeling and docking analysis revealed the molecular basis for the high catalytic activity of mutant LXCAR-S154Y toward BTAP. The results present here provide a promising alternative for economical and efficient production of chiral alcohols by engineered LXCAR.

Keywords Carbonyl reductase · *Leifsonia xyli* · Engineered enzyme · Directed evolution

N.-Q. Wang · J. Sun · J. Huang · P. Wang (✉)
College of Pharmaceutical Science, Zhejiang University of Technology, Hangzhou 310032, People's Republic of China
e-mail: wangpu@zjut.edu.cn

N.-Q. Wang
School of Life Science, Hunan University of Science and Technology, Xiangtan 411201, People's Republic of China

Introduction

Short-chain dehydrogenase/reductases (SDRs) are defined by a few sequence motifs and constitute one of the largest enzyme superfamilies of NAD(P)(H)-dependent oxidoreductases (Hoffmann and Maser 2007; Kallberg et al. 2002; Oppermann et al. 2003), which are distinctly different from functionally related enzymes such as medium-chain dehydrogenase/reductases (MDR) (Nordling et al. 2002) or aldo-keto reductase (AKR) (Hyndman et al. 2003). They have been found in all forms of life (archaea, bacteria and eukaryotes). Recently, SDRs have been highlighted as potential tools for their applications in biotechnology. For example, they have been used as biocatalysts to asymmetrically reduce some carbonyl compounds to their corresponding alcohols, which are widely used as building blocks in the synthesis of organic chemicals and chiral medicines (Liang et al. 2013; Lin et al. 2010; Rocha-Martín et al. 2012; Zhang et al. 2011; Zilbeyaz and Kurbanoglu 2010).

(*R*)-[3,5-bis(trifluoromethyl)phenyl] ethanol ((*R*)-BTPE) is a key chiral intermediate for the synthesis of Aprepitant (Emend®) and Fosaprepitant (Ivemend®), a tachykinin NK1 receptor antagonist widely administered to cancer patients without the nausea and vomiting side effects that often happen with chemotherapy (Jin et al. 2012; Nakade et al. 2008; Wu and Liaw 2012). Because of the increasing demand for (*R*)-BTPE, the search for novel approaches for economical

Published online: 01 May 2014

production of enantiomerically pure BTPE is becoming increasingly important. Previous research efforts that center on the biocatalytic asymmetric reduction of BTAP to (*R*)-BTPE have been reported by several groups (Gelo-Pujic et al. 2006; Homann et al. 2004; Kurbanoglu et al. 2009; Li et al. 2013).

Our previous study identified a novel *Leifsonia xyli* HS0904 showing asymmetrically catalytic activity capable of reducing 3,5-bis(trifluoromethyl) acetophenone (BTAP) to (*R*)-BTPE with excellent enantioselectivity and a yield of 62 % at 70 mM BTAP using glucose as cosubstrate (Wang et al. 2011). Moreover, a new carbonyl reductase derived from *L. xyli* HS0904 was purified and its biochemical properties were determined. This carbonyl reductase was found to have a broad spectrum of substrate specificity and asymmetrically catalyze the reduction of a variety of ketones and keto esters to their corresponding alcohols. Based on the N-terminal amino acid sequence, the obtained carbonyl reductase derived from *L. xyli* HS0904 probably belongs to the family of SDRs (Wang et al. 2013). Currently, by using isopropanol instead of glucose as cosubstrate for cofactor regeneration, *L. xyli* HS0904 was found to asymmetrically catalyze the reduction of BTAP to (*R*)-BTPE at 200 mM BTAP (51.2 g/l) with 91.8 % of product yield and 99.9 % of enantioselectivity (Ouyang et al. 2013). However, the relative low substrate concentration obtained in this study restricted its industrial scalization and limited its further application. Therefore, the development of more efficient and robust biocatalyst calls for novel molecular engineering approaches to improve the catalytic efficiency. The cloning and heterologous expression of enzymes in *Escherichia coli* cells are attractive methods to enhance enzyme production. Recently, recombinant *E. coli* used as whole-cell biocatalyst offers special advantage over conventional approaches. In particular, the use of recombinant cells coupled with cofactor regeneration greatly facilitated the industrial-scale biocatalytic process which usually requires significant substrate concentration of at least 100 g/l, a substrate to enzyme ratio of >50, and a conversion rate of >95 % (Huisman et al. 2010; Liang et al. 2009). Therefore, heterologous expression of *L. xyli* HS0904-derived carbonyl reductase in *E. coli* cells offers an alternative strategy for efficient synthesis of (*R*)-BTPE. Directed evolution strategies, such as error-prone polymerase chain reaction (epPCR), site-directed mutagenesis, site saturation mutagenesis, and DNA shuffling, are relatively simple and cost-effective approaches for protein evolution. These molecular engineering techniques have been successfully applied to tailor enzyme characteristics (Asako et al. 2008; Jakoblinnert et al. 2013; Machielsen et al. 2008; Wang et al. 2012).

In the present study, the carbonyl reductase derived from *L. xyli* HS0904 (LXCAR) was successfully overexpressed in *E. coli* BL21 (DE3). A mutant LXCAR-S154Y with enhanced catalytic activity was obtained by using epPCR and site-directed mutagenesis. This mutant exhibited the highest activity among all the tested enzyme variants. In addition, we performed kinetic analysis, structural modeling and docking studies to understand the structure-activity relationships of the enzyme. This work offers new possibilities for asymmetrical reduction of BTAP to (*R*)-BTPE by whole cells of engineered LXCAR.

Materials and methods

Chemicals

Restriction endonucleases, T4 DNA ligase, *Taq* DNA polymerase, *Pfu* DNA polymerase, and PrimeSTAR HS DNA polymerase were purchased from TaKaRa (Dalian, China). The bacterial genome DNA extraction, DNA gel extraction, and plasmid extraction kits were purchased from Axygen (Hangzhou, China). Kanamycin, ampicillin, and isopropyl-β-D-thiogalacto-pyranoside (IPTG) were purchased from Sigma-Aldrich. NADH disodium salt, protein molecular mass marker, and Bradford reagent came from Sangon Biotech Co., Ltd., Shanghai, China. (*R*)-BTPE and (*S*)-BTPE were purchased from Capot Chemical Co., Ltd., China. BTAP was provided by Beijing Golden Olive Company, China. The other chemicals used in this work were of analytical grade from local suppliers.

Strains, plasmids, and culture conditions

Strain *L. xyli* HS0904 has been deposited as CCTCC M 2010241 (Wang et al. 2011) and cultivated in a liquid medium as described by Wang et al. (Wang et al. 2013). The *E. coli* DH5α, *E. coli* BL21 (DE3) (Novagen, USA), plasmid pMD19-T (TaKaRa, Dalian, China), and pET-28a(+) (Novagen, USA) were used for gene cloning and recombinant protein expression experiments, respectively. *E. coli* cells were incubated in Luria-Bertani (LB) medium with an appropriate antibiotic if necessary as described by Sambrook and Russell (2001). All media were solidified with 2.0 % agar.

Enzyme assay and protein determination

LXCAR activity was assayed by measuring the decrease in the absorbance of NADH at 340 nm using BTAP as the substrate (Wang et al. 2013). The assay mixture consisted of 0.3 mM NADH, 10 mM BTAP, phosphate buffer (200 mM, pH 7.2), and 50 μl enzyme solution in a total volume of 2.5 ml. One unit of reductase activity was defined as the amount of enzyme that catalyzed the oxidation of 1 μmol NADH per min under the assay conditions. The blank was identical with the assay mixture except without the substrate (BTAP) addition. Protein content of samples was

quantified by the Bradford method (1976) using bovine serum albumin (BSA) as the standard.

Cloning of the LXCAR gene

The degenerate primers jbCAR-F1 and jbCAR-R1 (sequence shown in Table 1) were designed based on the N-terminal amino acid sequence of native LXCAR (AQYDVAGRSAI) described previously (Wang et al. 2013) and obtained internal amino acid sequences of LXCAR by trypsin-treated (VVAVGPGFIR), respectively. The genomic DNA of *L. xyli* HS0904 was extracted by the bacterial genome DNA extraction kit and used as a template for PCR amplification of the LXCAR gene. A 569-bp PCR fragment was obtained and then cloned into the plasmid pMD19-T for sequencing. The resulting sequence revealed high similarity with alcohol dehydrogenase from *Leifsonia* sp. S749. Therefore, a new set of degenerate primers jbCAR-F1/R2 (sequence shown in Table 1) was designed based on both end regions of alcohol dehydrogenase-encoding genes of *Leifsonia* sp. S749 (Inoue et al. 2006). PCR amplification was performed using the following reaction mixture (50 μl): 3 μl 25 mM $MgCl_2$, 4 μl 2.5 mM dNTP, 3 μl 100 pM each primer (jbCAR-F1 and jbCAR-R2), 1 μl 5 U/μl *Taq* DNA polymerase, 5 μl 10× PCR buffer, 10 ng DNA template from *L. xyli* HS0904, and 30 μl ddH_2O. The PCR parameters included an initial denaturation step at 95 °C for 5 min, followed by amplification of 30 s at 95 °C, 30 s at 55 °C, and 1 min at 72 °C for 30 cycles, and an elongation step at 72 °C for 10 min. Subsequently, PCR products were ligated into the plasmid pMD19-T and transformed into *E. coli* DH5α. Colonies with inserts were selected out by blue-white screening and colony PCR, following the sequence by Sangon Biotech Co., Ltd., Shanghai, China.

Table 1 Primers used in this study

Primers	Oligomeric sequences (5′–3′)
jbCAR-F1	5′-ATGGCNCARTAYGAYGTNGC-3′
jbCAR-R1	5′-ATGAANCCNGGNCCSACSGC-3′
jbCAR-R2	5′-YYAYTGNGCNGTRTAKCCYCC-3′
CAR-F	5′-CATGCCATGGCGCAGTACGACGTGG-3′
CAR-R	5′-CCCAAGCTTCTATTGTGCTGTGTAGCCTC-3′
S154Y-F	5′-GCCAACTATTCGGCGTACGTCACCGC-3′
S154Y-R	5′-GTACGCCGAATAGTTGGCGAAGCCGACGC-3′
L194I-F	5′-GCACCCCGATCGTGGCGTCGAACATGGAC-3′
L194I-R	5′-GACGCCACGATCGGGGTGCGGATGAAGC-3′

Underlined nucleotides represent the restriction sites

N for all bases, *R* for A or G, *Y* for T or C, *S* for G or C

Construction and sequencing of the expression vector

To construct the recombinant vector, the full LXCAR gene was amplified with the primers CAR-F and CAR-R which contained restriction sites of *Nco* I and *Hin*d III, respectively (sequence shown in Table 1). The PCR products were separated on a 1.0 % agarose gel and purified with a DNA gel extraction kit, and then digested with restriction endonucleases *Nco* I and *Hin*d III. The digested PCR products were purified and ligated into the plasmid pET-28a(+) digested with the same restriction endonucleases. The ligation mixture was transformed into *E. coli* BL21 (DE3) and plated onto LB agar plates containing 50 μg/ml kanamycin. The positive colonies were screened out by colony PCR, followed by double digestion of the recombinant vectors with *Nco* I and *Hin*d III, and then sequenced.

Expression of the recombinant LXCAR

Recombinant strain *E. coli* BL21 (DE3) harboring pET-28a(+)-*lxcar* were incubated in 50 ml LB medium containing 50 μg/ml kanamycin at 37 °C, 200 rpm for 12 h. Subsequently, the culture (1 % inoculum, *v*/*v*) was transferred into 500-ml Erlenmeyer flasks containing 100 ml of LB medium supplemented with 50 μg/ml kanamycin. Afterwards, 0.1 mM IPTG was added when the optical density at 600 nm (OD_{600}) reached 0.7 to induce the expression of the LXCAR. After further incubation at 30 °C for 10 h, cells were harvested by centrifugation at 12,000 rpm for 10 min; resuspended in phosphate buffer (200 mM, pH 7.2); and then disrupted by ultrasonication (400 W, pulse 2 s, pause 5 s) for 30 min. The intact cells and debris were removed via centrifugation at 4 °C, 12,000 rpm for 10 min, and the obtained supernatant was used as crude extract. Protein expression was visualized on 12 % (*w*/*v*) polyacrylamide gel according to the method of Laemmli (1970). The activity of crude extract was measured by the method described above.

Establishment of mutant library

A mutant library was established by in vitro directed evolution using epPCR. The PCR reaction mixtures (50 μl) were as follows: 3 μl 25 mM $MgCl_2$, 3 μl 5 mM $MnCl_2$, 1 μl 2.5 mM dNTP, 1 μl 10 mM dCTP, 1 μl 10 mM dTTP, 1 μl 100 pM each primer (CAR-F and CAR-R), 1 μl 5 U/μl *Taq* DNA polymerase, 5 μl 10× PCR buffer, 10 ng template DNA (the recombinant plasmid pET-28a(+)-*lxcar*), and 32 μl ddH_2O. The PCR conditions consisted of an initial denaturation step at 95 °C for 5 min, followed by amplification of 30 s at 95 °C, 30 s at 55 °C, and 1 min at 72 °C for 30 cycles, and an elongation step at 72 °C for 10 min. The target genes of approximately 0.75 kb were separated on a 1.0 % agarose gel and purified with a DNA gel extraction kit. The purified

DNA fragment was digested with *Nco* I and *Hin*d III, and ligated into the plasmid pET-28a(+) digested with the same restriction endonucleases. The resulting plasmids were transformed into *E. coli* BL21 (DE3) and plated onto LB agar plates containing 50 μg/ml kanamycin. The positive transformants were selected out by measuring the decrease in the absorbance of NADH at 340 nm using BTAP as the substrate and further confirmed by measuring the bioconversion rate of BTAP to (*R*)-BTPE with GC analysis.

Screening of mutants for improved LXCAR activity

Various single transformants were singled out from LB agar plates and incubated at 37 °C, 200 rpm for 12 h in 15-ml glass test tubes containing 5 ml LB medium supplemented with 50 μg/ml kanamycin. This was followed by transfer of the incubation solution (200 μl) into 15-ml glass test tubes containing 5 ml LB medium supplemented with 50 μg/ml kanamycin and incubation at 37 °C, 200 rpm for 6 h. Subsequently, 0.1 mM IPTG was added into the LB medium and further incubated for another 10 h to induce the expression of enzyme at 30 °C, 200 rpm. Cells were collected by centrifugation at 12,000 rpm for 10 min and subsequently lysed at 37 °C, 200 rpm for 2 h by the addition of 400 μl phosphate buffer (200 mM, pH7.2) containing 3 mg/ml lysozyme. The lysed cells were centrifuged at 12,000 rpm for 10 min, and the resulting supernatants were used to determine LXCAR activity by measuring the decrease in absorbance of NADH at 340 nm. Compared with parent recombinant *E. coli* cell supernatant, potential high-performance transformants were selected out and further confirmed by measuring the bioconversion rate of BTAP to (*R*)-BTPE with GC analysis.

The selected transformants were inoculated into 250-ml Erlenmeyer flasks containing 50 ml LB medium supplemented with 50 μg/ml kanamycin and incubated for 12 h at 37 °C, 200 rpm. The inoculum (1 %, *v*/*v*) was transferred into 500-ml Erlenmeyer flasks containing 100 ml of LB medium supplemented with 50 μg/ml kanamycin and further incubated at 37 °C, 200 rpm until OD_{600} reached 0.7. Subsequently, 0.1 mM IPTG was added to induce the expression of enzyme at 30 °C for 10 h. Cells were harvested by centrifugation (4 °C, 12,000 rpm, 10 min) and used as biocatalysts for asymmetric reduction of BTAP to (*R*)-BTPE. The reaction mixture contained 4.0 ml phosphate buffer (200 mM, pH 7.2), 1.0 ml isopropanol (20 %, *v*/*v*) as cosubstrate, certain amount of cells and substrate BTAP. The mixtures were incubated at 30 °C, 200 rpm for 1 h and were extracted with ethyl acetate. The product enantiomeric excess (ee) and conversion of the substrate were assayed by GC (Wang et al. 2011), and the positive transformants were confirmed compared with parent recombinant *E. coli* cells.

Site-directed mutagenesis

Site-directed mutagenesis was performed using S154Y-F/R and L194I-F/R primers (as shown in Table 1) to determine single amino acid substitution at positions 154 and 194 with tyrosine and isoleucine, respectively. Thirty PCR reactions were performed with PrimeSTAR HS DNA polymerase using recombinant plasmid pET-28a(+)-*lxcar* as the template DNA. The temperature program used was 2 min at 98 °C followed by 30 cycles of 10 s at 98 °C, 15 s at 55 °C, and 6 min at 72 °C and finished with 10 min at 72 °C. PCR amplification products were digested with *Dpn* I to remove parent plasmid (2 h at 37 °C with 10 units of *Dpn* I) and then transformed into *E. coli* BL21 (DE3) and plated on LB agar plates supplemented with 50 μg/ml kanamycin. The mutants LXCAR-S154Y (substitution of serine for tyrosine at position 154) and LXCAR-L194I (substitution of leucine for isoleucine at position 194) were screened out by colony PCR and then sequenced. The catalytic efficiencies of the mutants were confirmed by measuring the bioconversion rate of BTAP to (*R*)-BTPE with GC analysis.

Expression and purification of LXCAR mutants

Recombinant strain *E. coli* BL21 (DE3) harboring pET-28a(+)-*lxcar*-mutant were incubated at 37 °C in LB medium supplemented with 50 μg/ml kanamycin. IPTG was added to a final concentration of 0.1 mM for the induction of enzyme expression when the OD_{600} was about 0.7. After further incubation at 30 °C for 10 h, cells were harvested by centrifugation at 12,000 rpm for 10 min at 4 °C and then resuspended in Tris-HCl buffer (50 mM, pH 7.2) (buffer A) and disrupted by ultrasonication (400 W, pulse 2 s, pause 5 s) for 30 min. Cell debris was removed by centrifugation at 12,000 rpm for 10 min at 4 °C, and the obtained supernatant was used as crude extract.

The crude extract was fractionated with solid ammonium sulfate. The precipitate obtained with 30 to 60 % saturation of ammonium sulfate was collected, dialyzed with buffer A, and loaded onto a DEAE-Sepharose FF column (1.6 cm×20 cm, GE Healthcare Life Science, Piscataway, NJ, USA) previously equilibrated with buffer A. The enzyme was eluted with a linear 0- to 0.5-M NaCl gradient in buffer A. The fractions with high LXCAR activity were pooled, dialyzed with 0.5 M ammonium sulfate in buffer A, and applied onto an Octyl-Sepharose 4 FF column (1.6 cm×20 cm, GE Healthcare Life Science, Piscataway, NJ, USA) which had been pre-equilibrated with 0.5 M ammonium sulfate in buffer A, followed by elution with a linear 0.5- to 0-M ammonium sulfate gradient in buffer A. The collected fractions containing high LXCAR activity were dialyzed with buffer A and then loaded onto a High Q column (1.6 cm×20 cm, Bio-Rad) previously equilibrated with buffer A. The enzyme was eluted

with a linear gradient of NaCl from 0 to 1.0 M. Fractions with high LXCAR activity were collected and used as the purified enzyme for characterization.

Kinetic analysis

Kinetic parameters of the purified recombinant LXCAR and mutant LXCAR toward BTAP were determined in phosphate buffer (200 mM, pH 7.2) at 30 °C by increasing BTAP concentrations ranging from 1 to 10 mM at the same NADH concentration of 0.3 mM. Similarly, the kinetic parameters for NADH were also determined by increasing NADH concentrations ranging from 0.1 to 0.3 mM at the same BTAP concentration of 10 mM. The maximal reaction rate (V_{max}) and apparent Michaelis-Menten constant (K_m) were calculated based on the Lineweaver-Burk plot. The value of parameter k_{cat} was obtained by using the equation $k_{cat}=V_{max}/[E]$, where $[E]$ is the molar concentration of the enzymes.

Molecular homology modeling and docking

Three-dimensional homology models of LXCAR and LXCAR-S154Y were built based on the crystal structure of the SDR from *Sinorhizobium meliloti* 1021 (PDB ID: 3TOX) and oxidoreductase from *Thermus thermophilus* HB8 (PDB ID: 2D1Y) in complex with NADH using Build Homology Models, one of the modules in Discovery Studio 3.0 (Accelrys Inc., CA, USA). The generated model was then subjected to molecular mechanics optimization using CHARMM27 force field. Energy minimization was performed subsequently. The final models were checked using PROCHECK program (Laskowski et al. 1993), and the best quality model was chosen for further calculations, molecular modeling and docking studies by Discovery Studio 3.0.

Whole-cell bioreduction of aromatic ketone

The bioconversion of BTAP to (*R*)-BTPE using recombinant *E. coli* whole-cell biocatalyst was investigated. The incubated recombinant *E. coli* cells were harvested by centrifugation at 12,000 rpm for 10 min at 4 °C after expression of LXCAR and LXCAR-S154Y and washed twice with saline. The reaction mixture (5 ml) contained 4 ml phosphate buffer (200 mM, pH 7.2), 0.06 g *E. coli* cells (dry cell weight), 1 ml isopropanol (20 %, *v*/*v*) as cosubstrate, and certain amount of BTAP as substrate. The mixtures were incubated at 30 °C, 200 rpm, and sampled at regular time intervals. Samples were assayed for the product ee and conversion of BTAP by GC analysis after extraction with ethyl acetate (Wang et al. 2011).

Nucleotide sequence accession number

The nucleotide sequence data reported in this paper was deposited in the GenBank database with accession number of KF170285.

Results

PCR amplification, construction, and sequencing analysis of LXCAR gene

A 569-bp fragment was amplified using the primers jbCAR-F1/R1, and the sequence revealed high similarity with alcohol dehydrogenase from *Leifsonia* sp. S749 by sequence analysis. Subsequently, the degenerate primers jbCAR-F1 and jbCAR-R2 were designed to amplify the full LXCAR gene. As expected, a 756-bp fragment containing an intact open reading frame (ORF) was identified and cloned. The complete ORF contains both the ATG start codon and the TAG stop codon and encodes a protein with 251 amino acid residues. The deduced N-terminal amino acid sequence (AQYDVAGRS AI) and an internal sequence (VVAVGPGFIR) showed good agreement with the primer sequence (jbCAR-F1/R1). A web-based BLAST search revealed that the deduced amino acid sequence had 93 % identity with the hypothetical protein from *Leifsonia* sp. 109 (GenBank accession no. WP_018191686.1), 92 % identity with the hypothetical protein from *Cryocola* sp. 340MFSha3.1 (WP_020077127.1), and 89 % identity with the SDR from *Leifsonia* sp. S749 (BAD99642.1). It also exhibits 73 % identity with the hypothetical protein from *Microbacterium* sp. 292MF (WP_018172993.1) or *Rhodococcus* sp. 114MFTsu3.1 (WP_020112475.1), 72 % identity with the hypothetical protein from *Rhodococcus* sp. 29MFTsu3.1 (WP_019666994.1), and 71 % identity with the hypothetical protein from *Aeromicrobium* sp. JC14 (WP_019146152.1) or the putative oxidoreductase from *Rhodococcus* sp. AW25M09 (WP_008711153.1). Alignments of deduced amino acid sequences of the LXCAR gene are shown in Fig. 1.

Expression of the recombinant LXCAR

The full LXCAR gene (756 bp) was cloned into the pET-28a(+) vector and then introduced into competent *E. coli* BL21 (DE3). Recombinant cells harboring pET-28a(+)-*lxcar* could produce active LXCAR with IPTG induction, and the activity of recombinant *E. coli* crude extract was 1.54 U/mg, which was 62 times higher than that of *L. xyli* HS0904 crude extract (0.0249 U/mg). Sodium dodecyl sulfate polyacrylamide gel electrophoresis (SDS-PAGE) analysis of the crude extract showed that most of the recombinant LXCAR existed in soluble form (Fig. 2a). After purification by ammonium

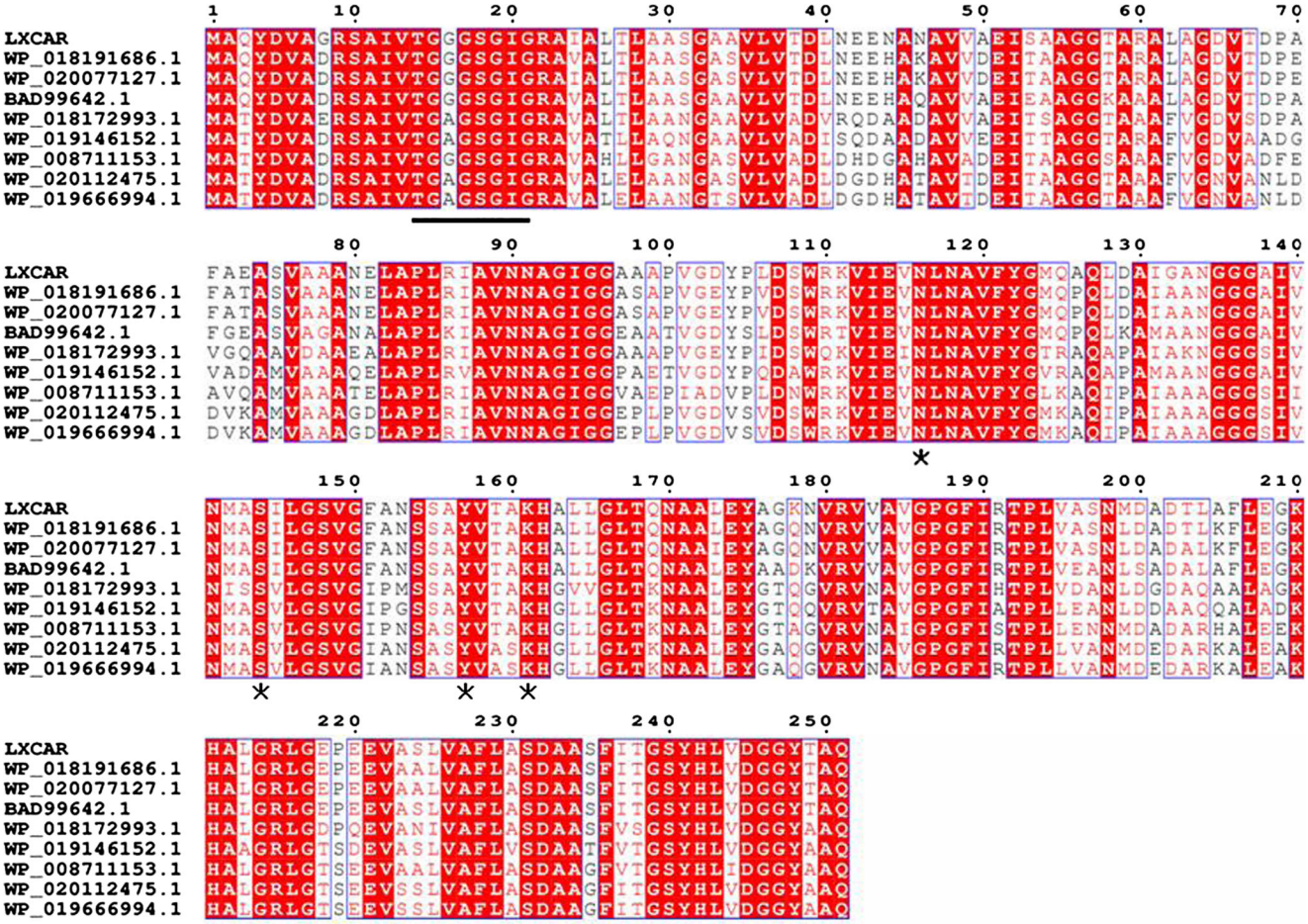

Fig. 1 Alignments of multiple amino acid sequences of LXCAR from *L. xyli* HS0904 and other proteins (indicated as the *GenBank accession number of each protein*). The N-terminal coenzyme-binding motif TGX_3GXG is indicated by *underlining*, and the catalytically active tetrad $NX_{27}SX_{12}YX_3K$ is indicated by *asterisks*

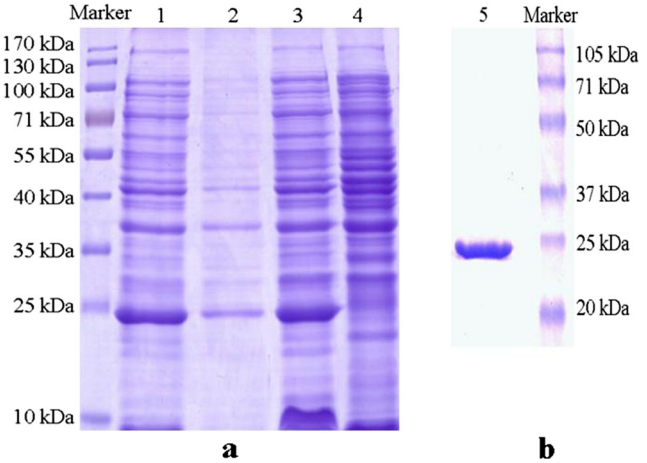

Fig. 2 SDS-PAGE analysis of soluble fractions obtained from expression experiments (**a**) and the purified LXCAR from the recombinant *E. coli* BL21 (DE3) (**b**). *Lane 1* indicates soluble fraction of crude extract of the recombinant *E. coli* BL21 (DE3) cells with IPTG induction, *lane 2* precipitated fraction of crude extract of the recombinant *E. coli* BL21 (DE3) cells with IPTG induction, *lane 3* the intact cells of the recombinant *E. coli* BL21 (DE3) cells with IPTG induction, *lane 4* the intact cells of the recombinant *E. coli* BL21 (DE3) cells without IPTG induction, and *lane 5* the purified LXCAR

sulfate precipitation, weak anion exchange chromatography on DEAE-Sepharose FF column, hydrophobic interaction chromatography on Octyl-Sepharose 4 FF column, and strong anion exchange chromatography on High Q column, a single band (about 24 kDa) on SDS-PAGE was observed (Fig. 2b), which corresponds to the recombinant LXCAR purified from the crude extract with the specific activity of 10.1 U/mg (Table 2). This result is consistent with our previous results (Wang et al. 2013).

Construction and screening of mutants

Random mutations were introduced into the LXCAR by epPCR to improve the LXCAR activity. Approximately 500 transformants were screened out, and five transformants showed higher LXCAR activity by determining the decrease in the absorbance of NADH at 340 nm using BTAP as the substrate. The obtained five transformants were further evaluated by measuring the bioconversion rate of BTAP to (*R*)-BTPE with GC analysis, and the best transformant (LXCAR-S154Y/L194I) with satisfactory yield was obtained. Sequence

Table 2 The specific activities of the recombinant LXCAR and its mutants

Types	Specific activities (U/mg)	Relative activities[a]
Recombinant LXCAR	10.1±0.3	1
LXCAR-S154Y/L194I	18.6±0.2	1.8
LXCAR-S154Y	23.4±0.4	2.3

[a] Relative to recombinant LXCAR

analysis indicated that four bases were replaced in this positive transformant: C461A, G462T, C580A, and C682T. Consequently, this corresponds to two amino acid replacements, namely, serine at 154 and leucine at 194, which were substituted with tyrosine and isoleucine, respectively.

To confirm the effects of each amino acid substitution individually and in combination, we reengineered the mutation sites into the LXCAR using site-directed mutagenesis. The results showed that the LXCAR-S154Y had higher activity than the LXCAR-S154Y/L194I and the LXCAR-L194I (data not shown). The LXCAR-S154Y and LXCAR-S154Y/L194I were purified from the crude extract by the method described above, and the specific activities toward BTAP were 23.4 and 18.6 U/mg, respectively (Table 2).

Kinetic analysis

Based on the Lineweaver-Burk plot, the K_m values and V_{max} values of the purified recombinant LXCAR, LXCAR-S154Y/L194I, and LXCAR-S154Y toward BTAP and NADH are estimated and summarized in Table 3. Compared with the recombinant LXCAR, the LXCAR-S154Y/L194I and LXCAR-S154Y showed higher affinity toward BTAP, as evidenced by the decrease in the K_m value and the increase in the k_{cat} value. Particularly, the LXCAR-S154Y/L194I and LXCAR-S154Y showed approximately 7.5-fold and 13-fold increase in the k_{cat}/K_m values compared to the recombinant LXCAR. Furthermore, the LXCAR-S154Y/L194I and LXCAR-S154Y also exhibited higher k_{cat}/K_m values toward NADH. These results indicated that the catalytic efficiency of engineered LXCAR was increased by the mutagenesis.

Bioreduction of BTAP to (*R*)-BTPE by whole cells of recombinant *E. coli*

To verify the potential of the LXCAR-S154Y as a biocatalyst, the bioconversion of BTAP to (*R*)-BTPE by whole cells of recombinant *E. coli* was tested at different substrate concentrations. As shown in Fig. 3, a best yield of 99.6 % for (*R*)-BTPE was attained for 2 h at 200 mM of BTAP, which was shortened by 2 h compared to the recombinant LXCAR. With a further increase of BTAP concentration up to 1,000 mM (256 g/l), a yield of 82.5 % for (*R*)-BTPE was achieved within 12 h, which was nearly 1.9-fold higher than the recombinant LXCAR. The product ee (>99 %) remained almost constant throughout the whole process (data not shown). These results suggested that *E. coli* whole cell expressing LXCAR-S154Y is a promising biocatalyst for future upscaling of the reductive conversion of BTAP to BTPE.

Discussion

In the present study, the gene encoding the LXCAR was successfully overexpressed in *E. coli* BL21 (DE3). This gene contained an open reading frame consisting of 756 nucleotides corresponding to 251 amino acid residues. A homology-based search of the deduced amino acid sequences of the LXCAR showed that it shared the highest similarity (93 % identity) with the hypothetical protein from *Leifsonia* sp. 109 (WP_018191686.1). It also exhibited 89 % identity with the SDR from *Leifsonia* sp. S749 (BAD99642.1) (Inoue et al. 2006). Moreover, two consensus sequences of the SDR family, an N-terminal TGX_3GXG cofactor-binding motif and a $SX_{12}YX_3K$ segment which is essential for catalytic activity of SDRs (Jörnvall et al. 1995), are fully conserved in the LXCAR (Fig. 1). Additionally, frequent sequence motifs of the SDRs were also found in the LXCAR, and details are shown in Table 4 (Oppermann et al. 2003). In our previous study, the LXCAR derived from *L. xyli* HS0904 is found to be a dimer protein comprised of two identical subunits of 24 kDa (Wang et al. 2013), which is different from the alcohol dehydrogenase (LSADH) involved in *Leifsonia* sp. S749 which is reported to be consisted of four identical subunits of 26 kDa

Table 3 Kinetic parameters of the purified recombinant LXCAR and its mutants toward BTAP and NADH

Types	BTAP				NADH			
	K_m (mM)	V_{max} (U mg^{-1})	k_{cat}[a] (s^{-1})	k_{cat}/K_m (s^{-1} mM^{-1})	K_m (mM)	V_{max} (U mg^{-1})	k_{cat}[a] (s^{-1})	k_{cat}/K_m (s^{-1} mM^{-1})
Recombinant LXCAR	0.573±0.008	10.9±0.5	21.1	36.8	0.025±0.007	12.2±0.7	23.6	944
LXCAR-S154Y/L194I	0.323±0.005	19.1±0.9	89.2	277	0.026±0.008	21.5±1.1	100	3,846
LXCAR-S154Y	0.201±0.006	24.7±1.2	114	463	0.029±0.011	26.6±0.9	122	4,207

[a] $k_{cat}=V_{max}/[E]$, where $[E]$ is the molar concentration of the enzymes

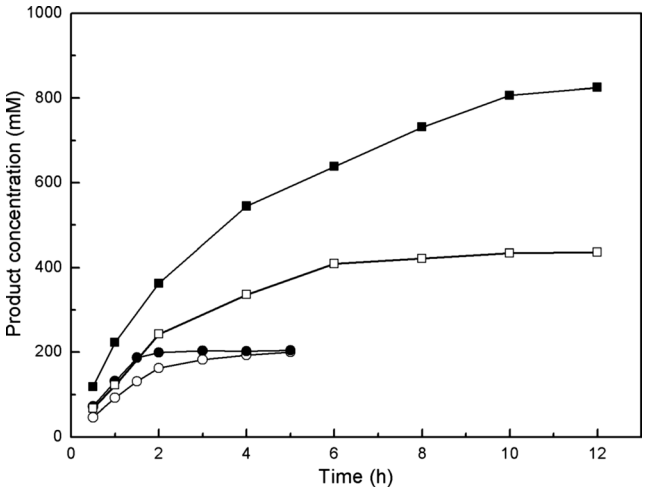

Fig. 3 Time course of asymmetric reduction of BTAP catalyzed by the recombinant LXCAR and LXCAR-S154Y whole cells, respectively. *Black circles* indicate 200 mM BTAP using the LXCAR-S154Y, *white circles* 200 mM BTAP using the recombinant LXCAR, *black squares* 1,000 mM BTAP using the LXCAR-S154Y, and *white squares* 1,000 mM BTAP using the recombinant LXCAR

(Inoue et al. 2005). Our results in this study further confirmed that the LXCAR derived from *L. xyli* HS0904 is a new member of the SDRs.

To improve the LXCAR activity, directed evolution was employed in the present work. Directed evolution is a simple and effective method for protein evolution. For example, directed evolution has been successfully employed to engineer proteins with diverse desired properties, such as activity (Gerstenbruch et al. 2012; Machielsen et al. 2008), enantioselectivity (Asako et al. 2008; Li et al. 2010), stability (Asako et al. 2008; Hoelsch et al. 2013; Jakoblinnert et al. 2013), and tolerance against organic solvents (Li et al. 2012). In our present study, a mutant LXCAR-S154Y with improved LXCAR activity toward BTAP was successfully obtained by epPCR and site-directed mutagenesis. This mutant demonstrated a 2.3-fold improvement in specific activity compared with the recombinant LXCAR (Table 2). To the best of our knowledge, this is the first reported case on improving the activity of SDRs from *Leifsonia* sp. by directed evolution. The finding of substitution of S154Y can enhance the enzymatic activity of SDRs, which is rarely ever reported.

Table 4 Sequence motifs found in LXCAR

Motif	Position	Function
TGX_3GXG	14–21	Coenzyme-binding region, maintenance of central β-sheet
D	65	Stabilization of adenine ring pocket, weak binding to coenzyme
NNAG	90–94	Stabilization of central β-sheet
N	116	Active site
S-Y-K	144,157,161	Active site
N	179	Connection of substrate-binding loop and active site
PG	187–188	Reaction direction
T	192	H bonding to carboxamide of nicotinamide ring

The previously determined N-S-Y-K residues constitute the active site in most SDR forms (Filling et al. 2002; Pace et al. 2011). All previous studies supported the concept that Tyr function acts as the catalytic base, whereas Ser stabilizes the substrate, Lys forms hydrogen bonds with the nicotinamide ribose moiety and lowers the pK_a of the Tyr-OH to promote proton transfer, and Asn stabilizes the position of Lys via a water molecule (Pace et al. 2011). In our present work, homology modeling and docking analysis were carried out to verify the hypothesis and explain the reaction mechanisms of the LXCAR-S154Y for asymmetric reduction of BTAP at the molecular level. Three-dimensional structure of the LXCAR-S154Y (Fig. 4a) was built based on the crystal structure of the SDR from *S. meliloti* 1021 (PDB ID: 3TOX) and oxidoreductase from *T. thermophilus* HB8 (PDB ID: 2D1Y) in complex with NADH, which have the highest sequence similarity to the LXCAR-S154Y in the PDB entries and shared 41 and 39 % identity, respectively. The RMSD value of modeled LXCAR was 1.322 Å. The LXCAR-S154Y structure was validated by Ramachandran plot using PROCHECK program (Fig. 4b). The plot revealed about 90 % of residues present in the most favored region and confirmed that the quality of the model is legitimate. Subsequently, docking studies of the LXCAR and LXCAR-S154Y complex with BTAP were carried out by flexible docking using Discovery Studio 3.0 (Fig. 5). The results showed that the carbonyl oxygen atom of BTAP, which is located close to the nicotinamide ring, forms hydrogen bonds with Tyr157 and Ser144. The C_4 atom of the nicotinamide ring may possibly donate its hydrogen atom to the carbonyl carbon atom of the BTAP. Moreover, the nicotinamide mononucleotide ring of the cofactor is located at the *si*-face of BTAP, and this ketone should be reduced to (*R*)-BTPE, which is consistent with our experimental results. Therefore, the LXCAR-S154Y as biocatalyst responsible for the anti-Prelog reduction of BTAP was testified, which is relatively rare since it is well recognized that most microorganisms/enzymes catalyzing ketone reduction followed Prelog's rule (Goldberg et al. 2007; Homann et al. 2004; Patel 2008).

The LXCAR-S154Y was also applied to asymmetrical reduction of BTAP to (*R*)-BTPE by *E. coli* whole-cell biocatalyst. A best yield of 99.6 % for (*R*)-BTPE was obtained for 2 h at 200 mM of BTAP, which was shortened by 28 and 2 h compared to *L. xyli* HS0904 and the recombinant LXCAR, respectively. The maximal (*R*)-BTPE concentration achieved 825 mM (82.5 % of yield) at 1,000 mM (256 g/l) of BTAP with above 99 % product ee within 12 h. To our knowledge, this is the highest substrate loading and product yield reported

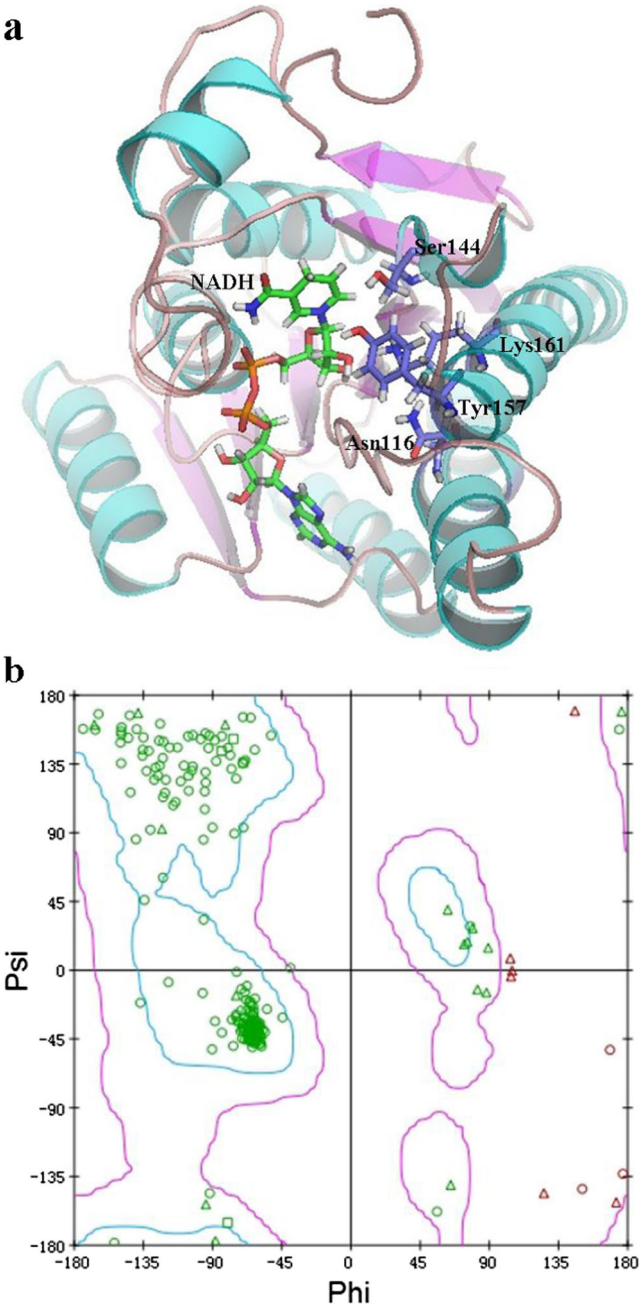

Fig. 4 The homology-modeled structure (**a**) and Ramachandran plot (**b**) of the LXCAR-S154Y. The NADH and the catalytic tetrad (N116, S144, Y157, and K161) are indicated by *green stick* and *blue stick*, respectively (**a**). The residues present in the most favored region and the disallowed region are indicated by *green* and *purple*, respectively (**b**)

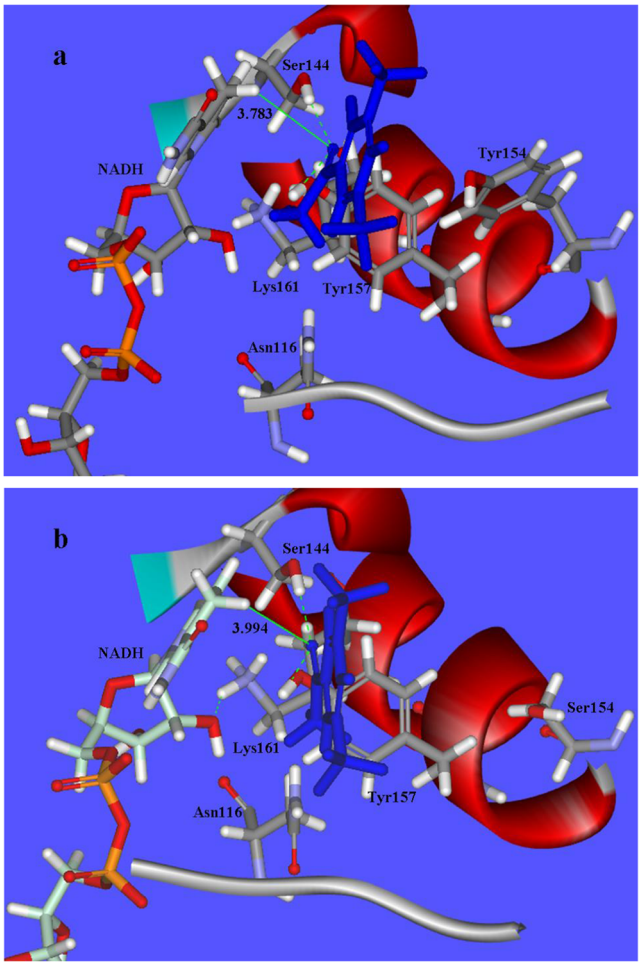

Fig. 5 Overlay of lowest energy docked conformations of BTAP (*dark blue*) with the conformations of the LXCAR-S154Y (**a**) and LXCAR (**b**) complex. The carbonyl oxygen atom of BTAP, which is located close to the nicotinamide ring, formed hydrogen bonds with Tyr157 and Ser144. The C_4 atom of the nicotinamide ring may possibly donate its hydrogen atom to the carbonyl carbon atom of the BTAP, with a distance of 3.99 and 3.78 Å between the C_4 atom and the carbonyl carbon in the conformations of the LXCAR and LXCAR-S154Y complex with BTAP. The binding energies of the LXCAR and LXCAR-S154Y complexes with BTAP were −10.3 and−79.3 kcal/mol, respectively. The nicotinamide mononucleotide ring of the cofactor is located at the *si*-face of BTAP. The Lys161 residue makes a hydrogen bond with the O2′ atom of the nicotinamide ribose moiety, and the O2′ atom donates hydrogen atoms to the OH atom of Tyr157

so far for the biocatalytic asymmetric reduction of BTAP to (*R*)-BTPE. The results indicated that the LXCAR-S154Y was an efficient and robust biocatalyst better than ever reported for the production of (*R*)-BTPE. In order to explain why the LXCAR-S154Y exhibited higher catalytic activity toward BTAP, the conformations of the LXCAR and LXCAR-S154Y complex with BTAP were analyzed. We found that the distances were 3.99 and 3.78 Å between the C_4 atom and the carbonyl carbon in the conformations of the LXCAR and LXCAR-S154Y complex with BTAP, respectively. Shortening of the distance means that it is more effective for an attack of a hydrogen atom from the C_4 atom of NADH against the carbonyl carbon atom of the substrate in transition states in the asymmetric reduction reaction. Moreover, the binding energies of the BTAP/LXCAR-S154Y complexes (−79.3 kcal/mol) were lower than those of the BTAP/LXCAR complexes (−10.3 kcal/mol). Additionally, the mutation binding energies and stability energies were also calculated by predicting stabilizing mutations at position

Ser154 with tyrosine substitution using Discovery Studio 3.0, and the values were −0.22 and −1.87 kcal/mol, respectively. Analysis of kinetics parameters also implied that the binding affinity of the LXCAR-S154Y to BTAP has been improved. Therefore, the LXCAR-S154Y exhibited higher reductive activity toward BTAP based on the above reasons.

In summary, the gene encoding the LXCAR has been successfully cloned from *L. xyli* HS0904 and overexpressed in *E. coli* BL21 (DE3). Moreover, the LXCAR-S154Y with higher LXCAR activity was obtained by directed evolution based on the epPCR and site-directed mutagenesis. This increase in catalytic activity is due to a single mutation outside the active site, revealing that there is still opportunity for further evolution of the enzyme toward higher activity or for other performance improvements. Meanwhile, our findings provide a promising platform for efficient synthesis of chiral intermediates of aprepitant and fosaprepitant by engineered LXCAR.

Acknowledgments This work was financially supported by grants from the National Natural Science Foundation of China (no. 21076193) and the Foundation of Zhejiang Educational Commission, China (no. Y201226056).

References

Asako H, Shimizu M, Itoh N (2008) Engineering of NADPH-dependent aldo-keto reductase from *Penicillium citrinum* by directed evolution to improve thermostability and enantioselectivity. Appl Microbiol Biotechnol 80:805–812

Bradford M (1976) A rapid and sensitive method for the quantitation of microgram quantities of protein utilizing the principle of protein-dye binding. Anal Biochem 72:248–252

Filling C, Berndt KD, Benach J, Knapp S, Prozorovski T, Nordling E, Oppermann U (2002) Critical residues for structure and catalysis in short-chain dehydrogenases/reductases. J Biol Chem 277:25677–25684

Gelo-Pujic M, Guyader FL, Schlama T (2006) Microbial and homogenous asymmetric catalysis in the reduction of 1-[3,5-bis(trifluoromethyl)phenyl] ethanone. Tetrahedron Asymmetry 17: 2000–2005

Gerstenbruch S, Wulf H, Mussmann N, O'Connell T, Maurer KH, Bornscheuer UT (2012) Asymmetric synthesis of D-glyceric acid by an alditol oxidase and directed evolution for enhanced oxidative activity towards glycerol. Appl Microbiol Biotechnol 96:1243–1252

Goldberg K, Schroer K, Lütz S, Liese A (2007) Biocatalytic ketone reduction—a powerful tool for the production of chiral alcohols—part I: processes with isolated enzymes. Appl Microbiol Biotechnol 76:237–248

Hoelsch K, Suhrer I, Heusel M, Weuster-Botz D (2013) Engineering of formate dehydrogenase: synergistic effect of mutations affecting cofactor specificity and chemical stability. Appl Microbiol Biotechnol 97:2473–2481

Hoffmann F, Maser E (2007) Carbonyl reductases and pluripotent hydroxysteroid dehydrogenases of the short-chain dehydrogenase/reductase superfamily. Drug Metab Rev 39:87–144

Homann MJ, Vail RB, Previte E, Tamarez M, Morgan B, Dodds DR, Zaks A (2004) Rapid identification of enantioselective ketone reductions using targeted microbial libraries. Tetrahedron 60:789–797

Huisman GW, Liang J, Krebber A (2010) Practical chiral alcohol manufacture using ketoreductases. Curr Opin Chem Biol 14:122–129

Hyndman D, Bauman DR, Heredia VV, Penning TM (2003) The aldo-keto reductase superfamily homepage. Chem Biol Interact 143:621–631

Inoue K, Makino Y, Itoh N (2005) Purification and characterization of a novel alcohol dehydrogenase from *Leifsonia* sp. strain S749: a promising biocatalyst for an asymmetric hydrogen transfer bioreduction. Appl Environ Microb 71:3633–3641

Inoue K, Makino Y, Dairi T, Itoh N (2006) Gene cloning and expression of *Leifsonia* alcohol dehydrogenase (LSADH) involved in asymmetric hydrogen-transfer bioreduction to produce (*R*)-form chiral alcohols. Biosci Biotechnol Biochem 70:418–426

Jakoblinnert A, van den Wittenboer A, Shivange AV, Bocola M, Heffele L, Ansorge-Schumacher M, Schwaneberg U (2013) Design of an activity and stability improved carbonyl reductase from *Candida parapsilosis*. J Biotechnol 165:52–62

Jin Y, Wu XM, Guan YM, Gu DY (2012) Efficacy and safety of aprepitant in the prevention of chemotherapy-induced nausea and vomiting: a pooled analysis. Support Care Cancer 20:1815–1822

Jörnvall H, Persson B, Krook M, Atrian S, Gonzalez-Duarte R, Jeffery J, Ghosh D (1995) Short-chain dehydrogenases/reductases (SDR). Biochemistry 34:6003–6013

Kallberg Y, Oppermann U, Jörnvall H, Persson B (2002) Short-chain dehydrogenase/reductase (SDR) relationships: a large family with eight clusters common to human, animal, and plant genomes. Protein Sci 11:636–641

Kurbanoglu EB, Zilbeyaz K, Taskin M, Kurbanoglu NI (2009) Total production of (*R*)-3,5-bistrifluoromethylphenyl ethanol by asymmetric reduction of 3,5-bis(trifluoromethyl)-acetophenone in the submerged culture of *Penicillium expansum* isolate. Tetrahedron Asymmetry 20:2759–2763

Laemmli UK (1970) Cleavage of structural proteins during the assembly of the head of bacteriophage T4. Nature 227:680–685

Laskowski RA, Macarthur MW, Moss DS, Thornton JM (1993) PROCHECK: a program to check the stereochemical quality of protein structures. J Appl Crystallogr 26:283–291

Li HM, Yang Y, Zhu DM, Hua L, Kantardjieff K (2010) Highly enantioselective mutant carbonyl reductases created via structure-based site-saturation mutagenesis. J Org Chem 75:7559–7564

Li J, Wang P, He JY, Huang J, Tang J (2013) Efficient biocatalytic synthesis of (*R*)-[3,5-bis(trifluoromethyl) phenyl] ethanol by a newly isolated *Trichoderma asperellum* ZJPH0810 using dual cosubstrate: ethanol and glycerol. Appl Microbiol Biotechnol 97: 6685–6692

Li ZW, Roccatano D, Lorenz M, Schwaneberg U (2012) Directed evolution of subtilisin E into a highly active and guanidinium chloride and sodium dodecylsulfate-tolerant protease. Chem Bio Chem 13:691–699

Liang J, Mundorff E, Voladri R, Jenne S, Gilson L, Conway A, Krebber A, Wong J, Huisman G, Truesdell S, Lalonde J (2009) Highly enantioselective reduction of a small heterocyclic ketone: biocatalytic reduction of tetrahydrothiophene-3-one to the corresponding (*R*)-alcohol. Org Process Res Dev 14:188–192

Liang P, Qin B, Mu M, Zhang X, Jia X, You S (2013) Prelog and anti-Prelog stereoselectivity of two ketoreductases from *Candida glabrata*. Biotechnol Lett 35:1469–1473

Lin WD, Chen CY, Chen HC, Hsu WH (2010) Enantioselective synthesis of (*S*)-phenylephrine by whole cells of recombinant *Escherichia coli* expressing the amino alcohol dehydrogenase gene from *Rhodococcus erythropolis* BCRC 10909. Process Biochem 45: 1529–1536

Machielsen R, Leferink NGH, Hendriks A, Brouns SJ, Hennemann HG, Daubmann T, van der Oost J (2008) Laboratory evolution of *Pyrococcus furiosus* alcohol dehydrogenase to improve the

production of (2S, 5S)-hexanediol at moderate temperatures. Extremophiles, 12:587–594

Nakade S, Ohno T, Kitagawa J, Hashimoto Y (2008) Population pharmacokinetics of aprepitant and dexamethasone in the prevention of chemotherapy-induced nausea and vomiting. Cancer Chemother Pharmacol 63:75–83

Nordling E, Jörnvall H, Persson B (2002) Medium-chain dehydrogenases/reductases (MDR). Eur J Biochem 269:4267–4276

Oppermann U, Filling C, Hult M, Shafqat N, Wu X, Lindh M, Jörnvall H (2003) Short-chain dehydrogenases/reductases (SDR): the 2002 update. Chem Biol Interact 143:247–253

Ouyang Q, Wang P, Huang J, Cai JB, He JY (2013) Efficient enantioselective synthesis of (*R*)-[3,5-bis(trifluoromethyl) phenyl] ethanol by *Leifsonia xyli* CCTCC M 2010241 using isopropanol as co-substrate. J Microbiol Biotechnol 23:343–350

Pace V, Cabrera ÁC, Ferrario V, Sinisterra JV, Ebert C, Gardossi L, Alcántara AR (2011) Structural bases for understanding the stereoselectivity in ketone reductions with ADH from *Thermus thermophilus*: a quantitative model. J Mol Catal B Enzym 70:23–31

Patel RN (2008) Synthesis of chiral pharmaceutical intermediates by biocatalysis. Coord Chem Rev 252:659–701

Rocha-Martín J, Vega D, Bolivar JM, Hidalgo A, Berenguer J, Guisán JM, López-Gallego F (2012) Characterization and further stabilization of a new anti-Prelog specific alcohol dehydrogenase from *Thermus thermophilus* HB27 for asymmetric reduction of carbonyl compounds. Bioresour Technol 103:343–350

Sambrook J, Russell DW (2001) Molecular cloning: a laboratory manual, 3rd edn. Cold Spring Harbor Laboratory, New York

Wang P, Cai JB, Ouyang Q, He JY, Su HZ (2011) Asymmetric biocatalytic reduction of 3,5-bis (trifluoromethyl) acetophenone to (1*R*)-[3, 5-bis(trifluoromethyl)phenyl] ethanol using whole cells of newly isolated *Leifsonia xyli* HS0904. Appl Microbiol Biotechnol 90: 1897–1904

Wang M, Si T, Zhao HM (2012) Biocatalyst development by directed evolution. Bioresour Technol 115:117–125

Wang NQ, Huang J, Luo HD, Wang P, Li J (2013) Purification and characterization of a new carbonyl reductase from *Leifsonia xyli* HS0904 involved in stereoselective reduction of 3,5-bis(trifluoromethyl) acetophenone. J Mol Catal B Enzym 92:1–6

Wu CE, Liaw CC (2012) Using aprepitant as secondary antiemetic prophylaxis for cancer patients with cisplatin-induced emesis. Support Care Cancer 20:2357–2361

Zhang RZ, Geng YW, Xu Y, Zhang WC, Wang SS, Xiao R (2011) Carbonyl reductase SCRII from *Candida parapsilosis* catalyzes anti-Prelog reaction to (*S*)-1-phenyl-1,2-ethanediol with absolute stereochemical selectivity. Bioresour Technol 102:483–489

Zilbeyaz K, Kurbanoglu EB (2010) Highly enantiomeric reduction of acetophenone and its derivatives by locally isolated *Rhodotorula glutinis*. Chirality 22:849–854